



The Society shall not be responsible for statements or opinions advanced in papers or discussion at meetings of the Society or of its Divisions or Sections, or printed in its publications. Discussion is printed only if the paper is published in an ASME Journal. Authorization to photocopy material for internal or personal use under circumstance not falling within the fair use provisions of the Copyright Act is granted by ASME to libraries and other users registered with the Copyright Clearance Center (CCC) Transactional Reporting Service provided that the base fee of \$0.30 per page is paid directly to the CCC, 27 Congress Street, Salem MA 01970. Requests for special permission or bulk reproduction should be addressed to the ASME Technical Publishing Department.

Copyright © 1997 by ASME

All Rights Reserved

Printed in U.S.A.

ANALYSIS OF INTERFACIAL CRACKS IN A TBC/SUPERALLOY SYSTEM UNDER THERMO-MECHANICAL LOADING

S. Q. Nusier and G. M. Newaz¹
Mechanical Engineering Department
Wayne State University
Detroit, Michigan 48202



ABSTRACT

In thermal barrier coatings (TBC) residual stresses develop during cool down from processing temperature due to the thermal expansion mismatch between the different layers (substrate, bond coat, and TBC). These residual stresses can initiate microcracks at the bond coat/TBC interface and can lead to debonding at the bond coat/TBC interface. The effect of voids or crack like flaws at the interface can be responsible for initiating debonding and accelerate the oxidation process. Effect of oxide layer growth between bond coat and ceramic layer (TBC) can be modeled as volume increase. In this work we represent this change in volume as an induced pressure across the interface. Mixed-mode fracture analysis of a thin circular delamination in an-axisymmetrically multi layer circular plate is developed. Geometrical nonlinearity is included in the analysis, since we have a large deflection case. The elastic deformation problem of a circular plate subjected to a clamped boundary condition at the edge of the delamination, an out of plane pressure load, and a compressive stress due to thermal mismatch between different layers, was solved numerically using a Rayleigh-Ritz method. The strain energy release rate was evaluated by means of the path-independent M -integral. The numerical results of this problem based on the energy method were verified using finite element method. Both methods correlate well in predicting the energy release rate for Mode I and Mode II, deflection, and postbuckling solutions. The energy release rates G , for both Mode I and Mode II using virtual crack extension method were evaluated. The specimen was cooled down from processing temperature of 1000 °C to 0 °C. The variation of the properties as a function of temperature was used for analysis. It was found that the use of temperature dependent properties in contrast to constant properties provides significantly different values of J -integral and G .

INTRODUCTION

Thermal barrier coatings (TBCs) provide thermal insulation and the bond coat provides oxidation resistance at high temperature to high temperature alloy substrates. Plasma-sprayed zirconia-yttria ceramic layer with a nickel-chromium-aluminum-yttrium bond coat on a substrate made of nickel-based superalloy (Chang, et al., 1987) is a common superalloy/TBC system. Application of these superalloy/TBC systems can be found in both aerospace and land-based gas turbine engines. In automotive applications, the piston head for diesel engine is coated to achieve longer life time and higher performance in terms of fuel reduction and power. However, these coatings have durability problems, due to the material and thermal mismatch between the coating and the metallic substrate. Thermal residual stresses develop during cool down from processing temperatures in TBC/metallic substrate. Environmental effects, specifically oxidation, create additional residual stresses due to the growth of an oxide layer causing additional material mismatch between the oxide surface and the TBC. These residual stresses may initiate microcracks such as debonding and radial cracks and can have profound effect on the response of the TBC and interfacial damage accumulation and failure. Their understanding is essential to predict the behavior of the coatings and their performance. The processing technique itself may produce voids or elongated flaws such as air bubble along the interfaces, which may initiate debonding.

Thermal fracture of multilayer ceramic thermal barrier coatings was studied by Takeuchi and Kokini (1994). The effect of a transient thermal load on a coating which is bonded to a cylindrical substrate was studied by Hornack and Kokini (1988). Finite element method was used to obtain a

¹Author receiving all communication

Presented at the International Gas Turbine & Aeroengine Congress & Exhibition
Orlando, Florida — June 2–June 5, 1997

This paper has been accepted for publication in the Transactions of the ASME
Discussion of it will be accepted at ASME Headquarters until September 30, 1997

solution for a circumferential edge crack normal to the coating. The finite element method has been used in conjunction with a numerical interface fracture mechanics model to investigate the structural response of coated brittle materials subjected to normal and shear loads, by Oneil and Wayne (1994). A finite element model to calculate the Mode II stress-intensity factors was developed by Van der Zande and Grootenboer (1986). The optimum size for a so-called singular element has been determined. Ahmad (1993) provides micromechanics based fracture analysis and correlation of experimental data for metal-ceramic and other interfaces. Suo (1995) studied wrinkles which induce interfacial stress and cause voiding. The strain energy release rate components G_I and G_{II} in Mode I and Mode II at the tip of an interface crack in a bimaterial plate under tension in a direction normal to the interface were evaluated using finite element analysis and modified crack closure integral (MCCI) technique by Dattaguru, et al., (1994). An elastoplastic solution for the interface crack with contact zones was studied by Aravas and Sharma (1991). Singular thermal stress fields in bonded viscoelastic quarter planes are studied by Blanchard and Ghoniem (1989). Singular stress and heat flux fields at the tip of the crack in a general nonhomogeneous material are studied by Jin and Noda (1994). New domain integrals for axisymmetric interface crack problems are derived by Nahta and Moran (1993). The effect of crack front curvature is shown to play an important role in the derivation of the integrals.

Descriptions of residual stresses and their influence on mechanical failure of coatings were studied by Evans, et al., (1983). The mechanics of the delamination and spalling of compressed films or coatings has been analyzed using a combination of fracture mechanics and post-buckling theory by Evans and Hutchinson (1984). The phenomenon of delamination buckling and growth in a time dependent radial compressive load is analyzed by Boltega and Maewal (1983). An iterative procedure based on the fourth-order Runge-Kutta integration formula is used to generate a family of nondimensionalized postbuckling solutions of von Karman's nonlinear plate theory by Yin (1985). A mixed-mode fracture analysis combining nonlinear thin-plate stress solutions with crack-tip elasticity results has been developed to account for local variations of G_I , G_{II} , and

G_{III} in thin-film debond problems associated with large film deformations by Chai (1990). A shaft-loaded blister test has been developed by Wan and Mai (1995) to measure the interfacial energy of a thin flexible polymeric film adhered to a rigid substrate. Expressions have been derived which describe the critical stress and pressure necessary to rupture oxide blisters which form on aluminum during growth of corrosion pits by Ryan and McCafferty (1995).

Although numerous efforts have been made to understand the effect of cracks on the life of TBC coated specimens, evolution and growth of the cracks still require special attention. It is now determined that in some TBC systems such as electron beam-plasma vapor deposition (EB-PVD), there is microcrack initiation. Microcracks coalesce to form major delamination cracks as reported by Newaz, et al., (1996). Interfacial crack in a layered disk specimen is shown in Fig. 1. An important consideration is the nature of crack growth characteristics at the TBC/bond coat interface. In a previous study by Nusier and Newaz (1996), it was shown that a central delamination under pure thermal loading has no stress intensification at the crack tip unless the delamination is large enough to promote buckling. By investigating the issue of interfacial crack growth, we will be able to evaluate the condition necessary for their growth under thermo-mechanical loading. This button specimen under consideration is amenable to axisymmetric modeling due to geometry. The importance of this problem is due to the fact that in order to achieve realistic prediction of TBC spallation performance, one needs to study the interaction of various layers and interfacial cracks at high temperature.

THEORETICAL AND COMPUTATIONAL ANALYSIS

The TBC coating in a button specimen as studied by Nusier and Newaz (1995) is in a state of biaxial compression. Residual compression stresses has been observed in TBC coating that was applied using Electron Beam-Plasma Vapor Deposition (EB-PVD) technique. This residual compression stress arise because of thermal expansion mismatch. Buckling failure mode has been observed by Newaz, et al. (1996) in the EB-PVD system. Oxidation growth between bond coat

and ceramic layer (TBC) can be modeled as volume increase which can be represented as an induced pressure across the interface (TBC/Oxide). Mixed-mode fracture analysis of a thin circular delamination in an-axisymmetrically multi layer circular plate is given as follows.

Theoretical Analysis

Let a circular plate of radius a be clamped at the edge of the delamination and subject to a uniformly distributed pressure p . The clamped edge has a radial displacement $\Delta \epsilon_0$ due to the applied compressive load (Fig. 1a). The deflection and slope at the clamped edge is zero, also the radial displacement at the center of the plate is zero. For a large deflection, the strain in the radial and the tangential direction are

$$\epsilon_r = \frac{du}{dr} + \frac{1}{2} \left(\frac{dw}{dr} \right)^2, \quad \text{and} \quad \epsilon_\theta = \frac{u}{r} \quad (1)$$

where u and w are the radial and vertical components of the displacement vector, respectively. Let N_r and N_θ be the corresponding tensile forces per unit length and applying Hooke's law, we obtain

$$N_r = \frac{Eh}{1-\nu^2} (\epsilon_r + \nu \epsilon_\theta), \quad \text{and} \quad N_\theta = \frac{Eh}{1-\nu^2} (\epsilon_\theta + \nu \epsilon_r) \quad (2)$$

where h is the TBC thickness, E is the TBC Young's modulus, and ν is the TBC Poisson's ratio. The strain energy due to bending is given by

$$V = \frac{D}{2} \int_0^{2\pi} \int_0^a \left[\left(\frac{\partial^2 w}{\partial r^2} \right)^2 + \frac{1}{r^2} \left(\frac{\partial w}{\partial r} \right)^2 + \frac{2\nu}{r} \frac{\partial w}{\partial r} \frac{\partial^2 w}{\partial r^2} \right] r dr d\theta \quad (3)$$

where D is the flexural rigidity of the plate, and is given by

$$D = \frac{Eh^3}{12(1-\nu^2)} \quad (4)$$

The strain energy due to stretching of the middle plane is

$$V_1 = 2\pi \int_0^a \left(\frac{N_r \epsilon_r}{2} + \frac{N_\theta \epsilon_\theta}{2} \right) r dr \quad (5)$$

The elastic deformation problem for a circular plate subjected to the boundary conditions indicated earlier was solved using a Rayleigh-Ritz method (an energy method) based on the following polynomial series solution

$$w = \sum_{i=1}^n c_i \left(1 - \frac{r^2}{a^2} \right)^{i+1}, \quad \text{and} \quad u = r(a^2 - r^2) \left(\sum_{i=1}^n b_i r^{2i-2} \right) - \epsilon_0 r \quad (6)$$

where c_i and b_i are constants to be evaluated from the condition that the total energy of the plate for a position of equilibrium is a minimum. Hence,

$$\frac{\partial V_1}{\partial b_i} = 0, \quad \text{and} \quad \frac{\partial(V + V_1)}{\partial c_i} \delta c_i = 2\pi \int_0^a p \delta w r dr \quad (7)$$

The first part of Eqn. 7 give us an n-linear equations for the constants b_i , these equations are solved in symbolic form, the second part of Eqn. 7 give us an n-nonlinear equations for the constants c_i , the solution of the constants b_i were used. All of this symbolic calculation are carried out by using Mathematica (1996). The set of nonlinear equations have been solved by IMSL (1989) library subroutine NEQNJ based on Levenberg -Marquardt algorithm with a user-supplied jacobian obtain by Mathematica also. The solution converged after 6 terms ($n=6$) for the case considered.

The compressive strain in the TBC layer can be obtained by applying the equilibrium radial force equation for the three layers. This solution is valid only for thick substrate. The radial stress in each layer is written in the following form

$$\begin{aligned} \sigma^c &= \frac{E^c}{1-\nu^c} [\varepsilon - \alpha^c (T - T_r)], \sigma^b = \frac{E^b}{1-\nu^b} [\varepsilon - \alpha^b (T - T_r)] \\ \sigma^s &= \frac{E^s}{1-\nu^s} [\varepsilon - \alpha^s (T - T_r)] \end{aligned} \quad (8)$$

where σ is the radial stress, α is the thermal expansion coefficient, and T_r is the stress free temperature, the superscript c , b , and s refers to TBC, bond coat and substrate, respectively. The equilibrium radial force equation for the three layers is

$$\sum F = \sigma^c A^c + \sigma^b A^b + \sigma^s A^s = 0 \quad (9)$$

Substituting Eqn. 8 into Eqn. 9, and solving for ε gives

$$\varepsilon = \frac{(\frac{E^c}{1-\nu^c} \alpha^c A^c + \frac{E^b}{1-\nu^b} \alpha^b A^b + \frac{E^s}{1-\nu^s} \alpha^s A^s)(T - T_r)}{\frac{E^c}{1-\nu^c} A^c + \frac{E^b}{1-\nu^b} A^b + \frac{E^s}{1-\nu^s} A^s} \quad (10)$$

Now, the compressive strain in TBC is

$$\varepsilon_0 = \varepsilon - \alpha^c (T - T_r) \quad (11)$$

In case of temperature dependent properties, the previous Eqns. 8-11 will be written in incremental form for each dT , then they will add up to get the right value of ε . For example, the variation of ε due to dT change in temperature will be given as

$$d\varepsilon = \alpha|_T (T - T_0) - \alpha|_{T-dT} (T - dT - T_0) \quad (12)$$

where T_0 is the reference temperature and is equal to zero.

Computational Fracture Analysis

Linear elastic fracture mechanics can be used to asses the conditions for crack growth of bimaterial interfaces. The mechanics of interface fracture can be traced back to the earlier works

of Griffith (1921) and Irwin (1960) on the general theory of fracture, of Williams (1959) on the elastic stress distribution around an interface crack, of England (1965), Erodogan (1965), and Rice and Sih (1965) on explicit solutions for interface cracks. The classical fracture mechanics concepts enable us to predict, without a detailed description of the crack tip processes, crack growth behavior in a fracture specimen. In recent years, complexity of obtaining closed-form solutions have been circumvented through computational fracture analysis to determine conditions for crack growth at bimaterial interfaces. However, the analytical basis is essential to study the critical parameters that characterize interface fracture.

Another approach to characterize fracture at bimaterial interface is via the J-integral. Originally developed by Eshelby (1956), the basic concept of J-integral is a path independent evaluation of the energy release rate. In other words, it is a measure of decrease in potential energy of the system with increase in crack length. In linear elastic fracture mechanics "J" is equivalent to G. The J-integral can be written as (Rice, 1968)

$$J = \int_{\Gamma} W dy - \int_{\Gamma} T \frac{\partial u}{\partial x} ds \quad (13)$$

where W is the strain energy density. Fig. 2 shows the notation and parameters for J-integral for a homogeneous medium. The analysis can be easily extended for a line crack between two materials assuming crack growth along the interface. The essence of J definition and its meaning remains unaltered for a crack at the bimaterial interface.

Following the work done by Yin (1985), the energy release rate associated with uniform-expansion growth of a circular delamination in a compressively loaded plate is obtained by means of the M-integral. The strain energy-release rate per unit increment of the area of delimitation is given by

$$G = \frac{1-\nu^2}{2Eh} \left\{ \left[\frac{Eh}{1-\nu} \varepsilon_0 - N_r(a) \right]^2 + 12 \left[\frac{M_r(a)}{h} \right]^2 \right\} \quad (14)$$

where $M_r(r)$ is given by

$$M_r(r) = D(w'' + \nu w' / r) \quad (15)$$

where the prime denote differentiation with respect to r .

For arbitrary combinations of N and M the stress field at the crack tip is governed by both K_I and K_{II} (Thouless, et al., 1987). Dimensional considerations require that the stress intensity factors be related to the load quantities by

$$K_I = d_1 N h^{-0.5} + d_2 M h^{-1.5}, \quad K_{II} = d_3 N h^{-0.5} + d_4 M h^{-1.5} \quad (16)$$

where the d_i are constants. The energy release rate is given by

$$G = \frac{(1-\nu^2)}{E} (K_I^2 + K_{II}^2) \quad (17)$$

Solving the crack problem for one loading combination and comparison of Eqns. 16 and 17 gives (Thouless, et al., 1987)

$$d_1 = 0.434, \quad d_2 = 1.934, \quad d_3 = 0.558, \quad d_4 = -1.503 \quad (18)$$

There is one idealized condition that we explored related to the specimen geometry. The presence of circumferential crack between the ceramic layer and the bond coat layer is as shown in Fig. 1 which was analyzed using finite element method. The general code ABAQUS (1995) was used for these analyses. The energy release rate G can be estimated by using the virtual crack extension method. The J-integral value can be found directly from ABAQUS.

Within linear elastic fracture mechanics two parameters are generally used to describe the conditions at the crack tip, normally the stress intensity factor(s) and the energy release rate. Evaluation of the stress intensity factor requires a thorough understanding of the state of stress at the crack tip. Energy release rate evaluation, on the other hand, is based more on an energy criteria and hence more popular.

A procedure for calculating the energy release rate, G , that has gained increasing acceptance over the past decade is the Virtual Crack Extension Method (VCEM). This was originally developed by Hellen and Parks (1975), who subsequently extended the method to cover material nonlinearities, and the evaluation of the J-integral. The strain energy release rate components G_I and G_{II} are calculated at the crack tip based on the Irwin's crack closure integral which primarily states that while considering a virtual crack extension method, the strain energy released is equal to the work done to close the crack back to the original size. The total strain energy release rate G_I could be evaluated through this integral by considering two problems with crack lengths of a & $a+da$ and finding the difference between their levels of strain energy. It can be seen that this method is very convenient to evaluate the individual strain energy release rate components, G_I and G_{II} in a mixed mode situation. Dattaguru, et al., (1994), used this method to evaluate the strain energy release rate components, G_I and G_{II} at bimaterial interface. Three models were used in their study, namely the bare interface model, the resin layer model and the subinterface crack model. The oscillatory singularity is not present in the resin layer model and in the subinterface crack model. For the case where the resin layer thickness and the distance between the subinterface crack and the interface are progressively decreased to an infinitesimally small value, they follow the trends of the bare interface model.

The method of VCE used to evaluate G is explained in the following few steps. The energy release rates in mode I and II are given by

$$G_I = \frac{1}{2A} f_x \Delta u_x, \quad G_{II} = \frac{1}{2A} f_y \Delta u_y \quad (19)$$

Where f_x and f_y are the reaction forces, A is the crack surface area corresponding to Δa , and similarly Δu_x and Δu_y are the difference in the displacements of nodes A and B in the x and y directions respectively (Figs. 3(a) & 3(b)).

The reaction forces and the displacements were obtained via two runs. For the first run, we assume a very weak spring, so the opening displacement and sliding displacement can be determined from springs deflection. In the second run the spring stiffness is assumed to be very high compared to the material stiffness, so the reaction forces can be determined. In this study a eight node isoparametric element are used, the energy release rates in mode I and mode II are given by

$$G_I = \frac{1}{2A} [f_{x1} \Delta u_{x1} + f_{x2} \Delta u_{x2}], \quad G_{II} = \frac{1}{2A} [f_{y1} \Delta u_{y1} + f_{y2} \Delta u_{y2}] \quad (20)$$

Hence

$$G_{total} = G_I + G_{II} \quad (21)$$

RESULTS AND DISCUSSION

The presence of circumferential crack between the ceramic layer and the bond coat layer as shown in Fig. 1 was analyzed using A Rayleigh-Ritz method and finite element method. The general code ABAQUS was used for finite element analysis. The energy release rate G was estimated by using the virtual crack extension method.

Finite element method was used in order to determine the J-integral value and the energy release rate. Virtual crack extension method was used to evaluate the energy release rate for both Mode I and Mode II crack growth. For layered disk specimen, the disk radius is 12.7 mm, the bond coat layer thickness is 0.04826 mm, the TBC thickness is 0.127 mm, and the uncoated Nickel based superalloy had a thickness of 3.175 mm. These dimensions are shown in Fig. 4. The properties of these three layers are given in Table 1. We analyzed a model case where the specimen was plasma sprayed in air with a thin zirconia-yttria ($ZrO_2 - 8wt\% Y_2O_3$) layer on a nickel-chromium-aluminum-zirconium bond coat, as in Ref. 1. The specimen was cooled down from a processing temperature of 1000 °C to a temperature of 0 °C. Half model for stepped-disk specimen was used since the specimen is axisymmetric. Eight node isoparametric element type was used; the total number of element was 1380. Along the longitudinal axis, the nodes can move in the axial direction only. The mesh was very fine close to the crack tip, and to make sure that the mesh is fine enough, another model with the same number of element but has one tenth of element size near to the crack tip, the difference in the results was less than 1%. Details of the finite element mesh near the crack tip is shown in Fig. 5.

Fig. 6 shows the variation of maximum deflection versus pressure ratio for a delamination radius of 20 times the TBC thickness. For zero pressure load the deflection has a value greater than zero due to early stage of buckling. At this stage the total energy release rate at crack tip may not be high enough for crack propagation. However as the coating deflection increases to gradual buckling and induced crack surface pressure, G_I may exceed the critical value that can cause crack growth. It is clear that the use of temperature dependent properties in contrast to constant properties provide significantly different values of maximum deflection. The finite element results compare to numerical results correlate very well. The variation of the maximum deflection versus pressure ratio is non-linear compare to linear variation as in the case of no geometrical nonlinearity. Using temperature dependent properties gives a 20-30% higher maximum deflection and energy release rate as seen in Figs. 6 and 7. The variation of J and G_I versus pressure ratio from finite element method and virtual crack extension method (VCEM) are shown in Fig. 7. Comparison between the energy release rate evaluated by energy method and by finite element method (J-integral) is shown in Fig. 8, finite element method and numerical method are in very good agreement.

Fig. 9 shows the variation of G_I and G_{II} versus pressure ratio for a delamination radius of twenty times the TBC thickness. This figure shows good agreement between finite element method results based on VCEM and numerical results. Mode I is dominant in this case. Fig. 10 is same as Fig. 9, but temperature dependent properties were used. In Fig. 10, we observe that Mode II energy release rate component is much smaller compared with the mode I component for both numerical and VCEM analyses. In either case, results match well. Figure 11 shows the variation of J-integral delamination radius from numerical analysis. From this figure one can obtain the conditions when the crack will propagate. From literature the critical energy release rate is varied between 100-300 J.m/m² for this system configuration. For a value of 300 J.m/m², and a delamination radius of four times the TBC thickness, the crack will propagate at induced pressure value equivalent to 500 atmosphere (≈ 50 MPa). This value is easy to develop due to volume increase because of oxide layer growth. Also, based on finite element analysis conducted by the authors for this system with a wavy interface, the results shows that an axial stress of 250 MPa can

be developed for a sine wave interface with amplitude of 2.4 μm and wave length of 127 μm . These values are practical for this system (Newaz, et al., 1996).

CONCLUSIONS

Effect of interfacial microcracks were investigated using fracture mechanics approach under thermo-mechanical loading. Thermal load was used in conjunction with internal surface induced pressure for interfacial cracks. The use of temperature dependent properties in contrast to constant properties provide significantly different values of J-integral and G values. Layered disk type specimen with a central crack has mixed mode conditions under thermo-mechanical loading. The total energy release rate evaluated by the virtual crack extension method and the J-integral value evaluated directly by ABAQUS agree quite well. The maximum deflection and total energy release rate evaluated by finite element method and energy method are in very good agreement.

For a TBC toughness value of 300 J.m/m^2 , and a delamination radius of four times the TBC thickness, the crack will propagate at induced pressure value equivalent to 500 atmosphere (≈ 50 MPa). The results clearly indicate that small internal pressure due to oxidation induced volume change may create the necessary conditions for crack growth during thermal cycling. This value may easily develop due to volume increase because of oxide layer growth or due to the presence of a wavy interface.

ACKNOWLEDGMENT

Funding for this research was provided through a grant (# F49620-95-1-0201) from the Air Force Office of Scientific Research (AFOSR). Dr. Walter Jones is the program monitor. Discussion and interaction with Dr. P. K. Wright of GEAE is gratefully acknowledged.

REFERENCES

- Ahmad, J., 1993, "A Micromechanics Based Representation of Combined Mode I and Mode II Toughness of Brittle Materials and Interfaces," *ASME J. of Engineering Materials and Technology*, vol. 115, 101-105.
- ABAQUS, 1995, Hibbit, Karlsson and Sorensen, Inc.
- Aravas, N., and Sharma, S. M., 1991, "An Elastoplastic Analysis of the Interface Crack with Contact Zones", *J. Mech. Phys. Solids* Vol. 39, No. 3, 311-344.
- Blanchard, J. P., and Ghoniem, N. M., 1989, "Relaxation of Thermal Stress Singularities in Bonded Viscoelastic Quarter Planes", *Transactions of the ASME*, 56, 756-762.
- Bottega, W. J., and Maewal, A., 1983, "Delamination Buckling and Growth in Laminates", *Transactions of the ASME*, Vol. 50, 184-189.
- Bottega, W. J., and Maewal, A., 1983, "Dynamics of Delamination Buckling", *Int. J. Non-Linear Mechanics*, Vol. 18, No. 6, 449-463.
- Chai, H., 1990, "Three-Dimensional Fracture analysis of Thin-Film Debonding", *Int. J. Fracture*, Vol. 46, 237-256.
- Chang, G. C., and Phucharoen, W., Miller, R. A., 1987, "Finite Element Thermal Stress Solutions for Thermal Barrier Coatings", *Surface and Coatings Technology*, 32, 307-325.
- Dattaguru, B., Venkatesha, K. S., Ramamurthy, T. S., and Buchholz, F. G., 1994, "Finite Element Estimates of Strain Energy Release Rate Components at the Tip of an Interface Crack Under Mode I Loading", *Engineering Fracture Mechanics*, Vol. 49, No. 3, 451-463.
- Dundurs, J., 1969, Discussion, *J. Appl. Mech.*, 36, p. 650.
- England, A. H., 1965, "A Crack Between Dissimilar Media", *J. Appl. Mech.* 32:400-402
- Erdogan, F., 1965, "Stress Distribution in Bonded Dissimilar Materials With Cracks", *J. Appl. Mech.* 32:403-410.
- Eshelby, J. D., 1956, "The Continuum Theory of Lattice Defects, in *Solid state Physics*, 3, 79-141.
- Evans, A. G., Crumely, G. B., and Demaray, R. E., 1983, "On the Mechanical Behavior of Brittle Coatings and Layers", *Oxidation of Metals*, Vol. 20, No. 5/6.

TABLE 1
Material properties at 22 & 566 & 1149 °C

Material	Young's modulus (GPa)	Poisson's ratio	Coefficient of thermal expansion (°C ⁻¹)
Substrate	175.8	0.25	13.91 x 10 ⁻⁶
	150.4	0.2566	15.36 x 10 ⁻⁶
	94.1	0.3224	19.52 x 10 ⁻⁶
Bond coat	137.9	0.27	15.16 x 10 ⁻⁶
	121.4	0.27	15.37 x 10 ⁻⁶
	93.8	0.27	17.48 x 10 ⁻⁶
TBC	27.6	0.25	10.01 x 10 ⁻⁶
	6.9	0.25	11.01 x 10 ⁻⁶
	1.84	0.25	12.41 x 10 ⁻⁶

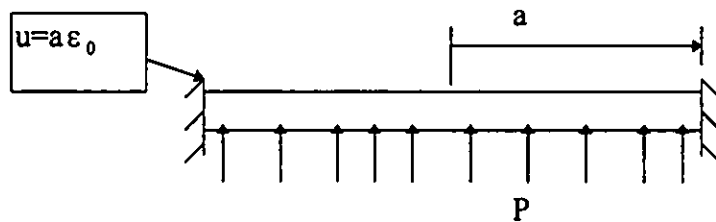


Figure 1a. Circular plate under uniform pressure and edge displacement of $a\epsilon_0$

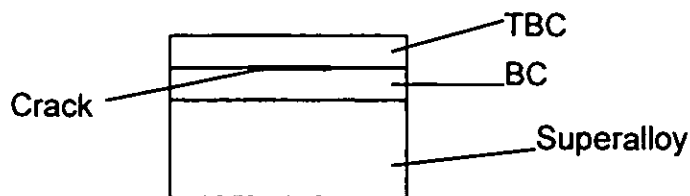


Figure 1b. Circumferential crack between the ceramic layer and the bond coat layer in a stepped-disk specimen.

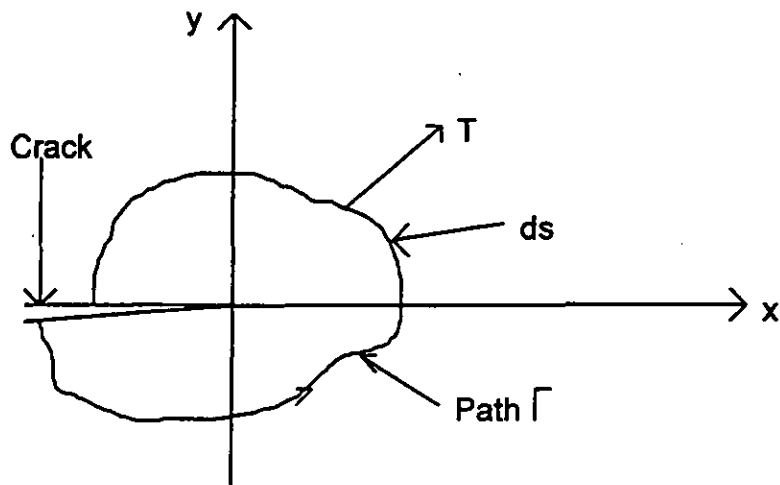


Figure 2. Notation and parameters used for J-integral.

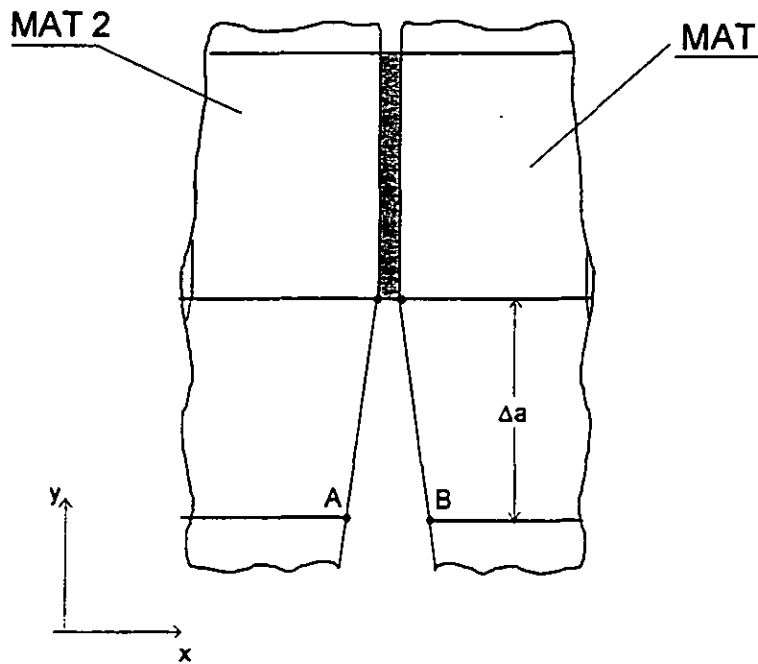


Figure 3a. Interfacial crack between bond coat and TBC.

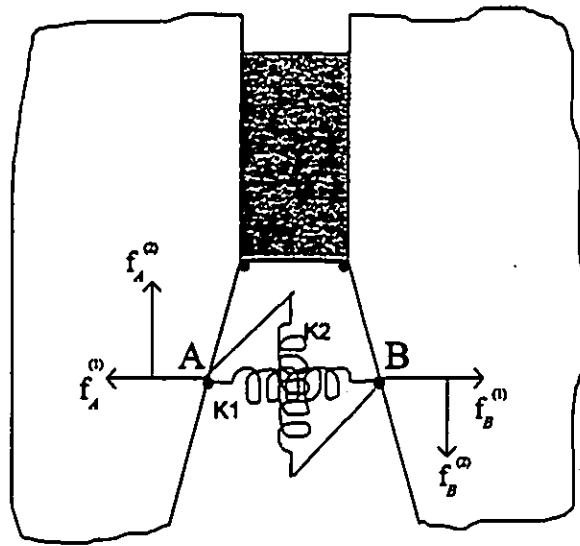


Figure 3b. Forces and displacement illustrations for a crack.

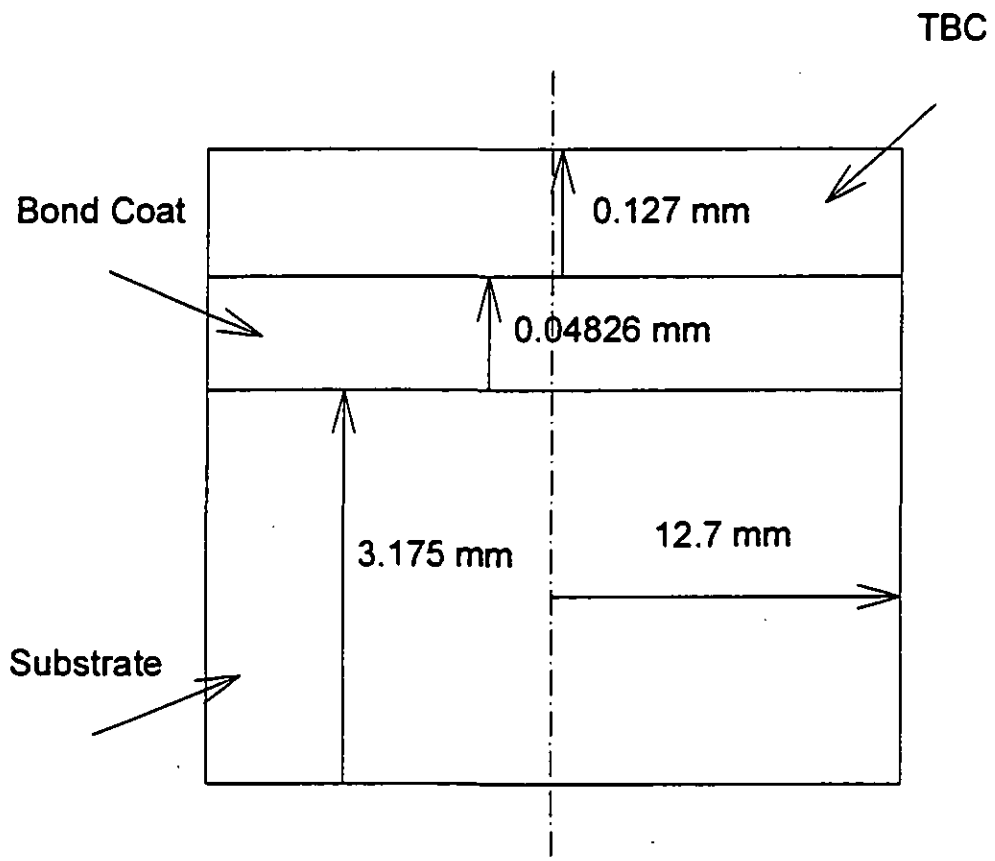


Figure 4. Dimension of TBC layer in relation to bond coat and superalloy substrate.

- Evans, A. G., and Hutchinson, J. W., 1984, "On the Mechanics of Delamination and Spalling in Compressed Films", *Int. J. Solids Structures*, Vol. 20, No. 5, 455-466.
- Griffith, A. A., 1921. *Phil. Trans. Roy. Soc. Lond.* A221:163-197.
- Hellen, T. K., 1975, "On the Method of Virtual Crack Extensions", *Int. J. Num. Meth.* 9, 187-207.
- Imsl, 1989, *User's Manual*, Houston, Texas, version 1.0.
- Irwin, G. R., 1960. In: *Structural Mechanics*. (J. N. Goodier and N. J. Hoff, eds.), 557-591, Oxford: Pergamon Press.
- Jin, Z., and Noda, N., 1994, "Crack-Tip Singular Fields in Nonhomogeneous Materials", *Transactions of the ASME*, 61, 738-740.
- Kokini, K., and Hornack, T. R., 1988, "Transient Thermal Load Effects on Coatings Bonded to Cylindrical Substrates and Containing Circumferential Cracks", *J. of Eng. Mat. and Tech.*, 110, 35-40
- Mathematica, 1996, Wolfram Media, Inc., version 3.
- Nahta, R., and Moran, B., 1993, "Domain Integrals For Axisymmetric Interface Crack Problems", *Int. J. Solids Structures*, Vol. 30, No. 15, 2027-2040.
- Newaz, G. M., Nusier, S. Q., Chaudhury, Z. A., and Wright, K. P., 1996, "Damage Accumulation Mechanisms in Thermal Barrier Coatings", To be presented at IMECE'96, Atlanta.
- Nusier, S. Q., Newaz, G. M., 1996, "Analysis of Interfacial cracks in a TBC/Superalloy System under Thermal Loading", submitted to *J. of Engineering Fracture Mechanics*.
- Oneil, D. A., and Wayne, S. F., 1994, "Numerical Simulation of Fracture in Coated Brittle Materials Subjected to Tribo-Contact", *J. of Eng. Mat. and Tech.* 116, 471-478.
- Rice, J. R., 1988, "Elastic Fracture Mechanics Concepts of Interfacial Cracks", *J. Appl. Mech.*, 55, p. 98-103.
- Rice, J. R., 1968, "Mathematical Analysis in the Mechanics of Fracture, in *Fracture*", An Advanced Treatise (editor H. Leibowitz), Academic Press, New York, 2, pp. 191-311.
- Rice, J. R., and G. C. Sih., 1965, "Plane Problems of Cracks in Dissimilar Media", *J. Appl. Mech.* 32:418-423.
- Ryan, R. L., and McCafferty, E., 1995, "Rupture of an Oxide Blister", *J. Electrochem. Soc.*, Vol. 142, No. 8, 2594-2597.
- Suo, Z., 1995, "Wrinkles of the Oxide Scale on an Aluminum-Containing Alloy at High Temperature", *J. of Mechanics of Physics and Solids*, Vol. 43, No. 6, 829-846.
- Takeuchi, Y. R., and Kokini, K., 1994, "Thermal Fracture of Multilayer Ceramic Thermal Barrier Coatings", *J. of Eng. for gas Turbs. and power. Transactions of the ASME*, 116, 266-271
- Thouless, M. D., Evans, A. G., Ashby, M. F., and Hutchinson, J. W., 1987, "The Edge Cracking and Spalling of Brittle Plates", *Acta Metall.* Vol. 35, No. 6, 1333-1341.
- Van der Zande, H. D., and Grootenboer, H. J., 1986, "A Finite Element Approach to Interface Cracks", *J. of App. Mechs.*, 53, 573-578.
- Wan, K. and Mai, Y., 1995, "Fracture Mechanics of a Shaft-Loaded Blister of Thin Flexible Membrane on Rigid Substrate", *Int. J. Fracture*, Vol. 74, 181-197.
- Williams, M. L., 1959, "The Stresses Around a Fault or Crack in Dissimilar Media", *Bull. Seismol. Soc. Am.* 49:199-204.
- Yin, W., 1985, "Axisymmetric Buckling and Growth of a Circular Delamination in a Compressed Laminate", *Int. J. Solids Structures*, Vol. 21, No. 5, 503-514.